Nitrogen-doped graphene and its electrochemical applications†

Yuyan Shao,[a] Sheng Zhang,[a] Mark H. Engelhard,[a] Guosheng Li,[a] Guocheng Shao,[a] Yong Wang,[ab] Jun Liu,[a] Ilhan A. Aksay[c] and Yuehe Lin*[a]

Received 21st March 2010, Accepted 4th June 2010
DOI: 10.1039/c0jm00782j

Nitrogen-doped graphene (N-graphene) is obtained by exposing graphene to nitrogen plasma. N-graphene exhibits much higher electrocatalytic activity toward oxygen reduction and H_2O_2 reduction than graphene, and much higher durability and selectivity than the widely-used expensive Pt for oxygen reduction. The excellent electrochemical performance of N-graphene is attributed to nitrogen functional groups and the specific properties of graphene. This indicates that N-graphene is promising for applications in electrochemical energy devices (fuel cells, metal–air batteries) and biosensors.

1. Introduction

Graphene, a two-dimensional carbon material with atoms arranged in a honeycomb lattice, has attracted strong scientific and technological interests[1] because of its unique physical/chemical properties (high surface area,[1] excellent conductivity,[1] and mechanical strength,[2] *etc.*) and potential low production cost.[1,3] Graphene has shown great application potential in many fields, such as electronics,[4] energy,[5–9] and biotechnology.[10–13]

Theoretical[14,15] and experimental[16–20] studies have shown that doping graphene can tailor the physical/chemical properties of graphene and open the possibilities of new chemistry and new physics on graphene. For example, nitrogen doping can tune the chemically derived functionalized graphene from being a p-type[21] to n-type semiconductor.[16] Graphene is a basic building block for graphitic materials of all other dimensionalities (0D fullerenes, 1D nanotubes, and 3D graphite),[1] and studying doped graphene is expected to provide fundamental insight into doped carbon materials.

In fact, doping is a common strategy in tuning the properties of carbon nanotubes (CNTs)[22] which are rolled-up graphene sheets. Nitrogen-doped CNTs (N-CNTs) have shown promise in electrochemistry; for example, N-CNTs greatly increase oxygen reduction kinetics which is of great significance in fuel cells,[23,24] and they have also shown excellent biosensing performance.[25] Graphene and its nanocomposites have also been developed for biosensors,[11,13,26–29] and graphene also exhibits electrocatalytic activity for oxygen reduction.[30,31]

Numerous methods have been developed to produce graphene (or graphene sheets),[32] including mechanical exfoliation of graphite with scotch tape,[33] mild exfoliation of graphite,[34] chemical vapor deposition (CVD),[35] chemical[36,37]/electrochemical[38]/thermal[3]/solvothermal[39] reduction of graphite oxide (GO). However, only a few methods have been developed to produce nitrogen-doped graphene (N-graphene). Wang *et al.*[16] reported that n-type electronic doping of graphene with nitrogen can be obtained by high-power electrical annealing (e-annealing) in NH_3. Li *et al.*[18] produced N-graphene by thermal annealing of graphene oxide in ammonia which realized simultaneous nitrogen doping and the reduction of graphene oxide. Qu *et al.*[20] reported N-graphene produced from CVD of methane in the presence of ammonia. N-graphene has also been prepared by direct current arc-discharge between pure graphite electrodes with NH_3[40] or pyridine vapor[41] as the nitrogen source.

Here, we report the production of N-graphene from nitrogen plasma-treated graphene and its electrochemical applications. Qu *et al.*[42] report the high electrocatalytic activity of N-graphene, which was synthesized with the CVD method, toward oxygen reduction. Our graphene reported here was prepared through the rapid thermal expansion of graphite oxides (see refs. 3 and 43 for details on the synthesis and characterization of graphene), which in general we refer to as functionalized graphene sheet (FGS) due to the oxygen functional groups and lattice defects on them.[44] However, in the rest of this paper, to distinguish FGS from N-graphene, we will simply refer to it as graphene. This material is now also available in large quantities from Vorbeck Materials Corp. (Jessup, MD, USA). N-graphene was synthesized by exposing FGS to nitrogen plasma, which is a facile method in doping graphene and through which N-doping can be easily controlled, for example, N content can be easily controlled by changing the plasma strength and/or exposure time.

Oxygen and hydrogen peroxide were employed as the probe molecules to study the electrocatalytic behavior of N-graphene. The oxygen reduction reaction (ORR) is a key reaction in many electrochemical energy devices such as fuel cells and metal–air batteries. In fuel cells, Pt nanocatalysts are usually used for oxygen reduction, which are limited by cost and durability issues.[45] Searching for highly active, low-cost and durable electrocatalytic materials, especially those to replace Pt,[46] has always been the hot topic for chemists and materials scientists.[47–49] H_2O_2 is a general enzymatic product of oxidases and a substrate of peroxidases, which are important in biological processes and

[a]*Pacific Northwest National Laboratory, Richland, WA 99352, USA. E-mail: yuehe.lin@pnl.gov*
[b]*The Gene and Linda Voiland School of Chemical Engineering and Bioengineering, Washington State University, Pullman, WA 99164, USA*
[c]*Department of Chemical and Biological Engineering, Princeton University, Princeton, NJ 08544, USA*

† Electronic supplementary information (ESI) available: TEM images of graphene and N-graphene, oxygen reduction polarization curves, electrochemical behaviors and XPS of oxygen plasma-treated graphene (O-graphene). See DOI: 10.1039/c0jm00782j

biosensors.[50] H_2O_2 is also an essential mediator in food, pharmaceutical, clinical, industrial, and environmental analysis.[27] Therefore, it is important to test H_2O_2. N-graphene exhibits greatly enhanced electrocatalytic activity toward both ORR and H_2O_2 reduction and shows potential applications in electrochemical energy devices and biosensors. The 2D structure of N-graphene (and graphene in general) is also expected to make the ohmic resistance (mainly from contact resistance[51]) much lower if assembled into electrodes due to the excellent contact of graphene (it is reasonable that 2D structured materials usually have better contact than 1D structured materials and particles because of the larger contact area between graphene).

2. Experimental

Graphene synthesis

The synthesis of graphene used in this study has been reported previously.[3,43] In brief, natural flake graphite was first oxidized in a strong oxidizing solution of concentrated sulfuric acid, concentrated nitric acid, and potassium chlorate. The resultant graphite oxide was dried and rapidly heat-treated (>2000 °C/min) in an argon-filled fused silica tube to 1050 °C to split the graphite oxide into wrinkled graphene sheets through evolution of CO_2.

Nitrogen doping

Graphene was dispersed in ethanol and then applied onto pre-cleaned glassy carbon (GC). After drying, graphene was firmly attached onto GC and covered all the surface of GC. Then, graphene on GC was placed into the plasma chamber (PC2000 – Plasma Cleaner, South Bay Technology, Inc.). The chamber pressure was pumped down to 50 mTorr, and then nitrogen was introduced into the chamber to create plasma by applying a radio-frequency (13.56 MHz) forward power of 140 W (the reflection power <3 W) for 20 min. The chamber pressure was 200 mTorr. The DC bias was 990 V. Oxygen plasma-treated graphene (O-graphene) was also prepared for comparison with the similar protocol.

Materials characterization

The X-ray photoelectron spectroscopy (XPS) characterization was carried out on a Physical Electronics Quantum 2000 Scanning ESCA Microprobe with a 16 element multichannel detector. This system uses a focused monochromatic Al Kα X-ray (1486.7 eV) source and a spherical section analyzer. The X-ray beam used was a 100 W, 100 μm diameter beam that was rastered over a 1.3 mm × 0.2 mm rectangle on the sample. The X-ray beam is incident normal to the sample and the photoelectron detector was at 45° off-normal using an analyzer angular acceptance width of 20° × 20°. Wide-scan data were collected using a pass energy of 117.4 eV. For the $Ag3d_{5/2}$ line, these conditions produce FWHM of better than 1.6 eV. High energy resolution spectra were collected using a pass energy of 46.95 eV. For the $Ag3d_{5/2}$ line, these conditions produced FWHM of better than 0.98 eV. The binding energy (BE) scale was calibrated using the $Cu2p_{3/2}$ feature at 932.62 ± 0.05 eV and Au4f at 83.96 ± 0.05 eV for known standards. Raman spectra of samples were taken on a Renishaw 1000 microspectrometer using an excitation wavelength of 514.5 nm.

Electrochemical tests

All the electrochemical tests were carried out in a standard three-electrode cell with a Pt wire as the counter electrode. The electrochemical cell was controlled with a CHI 660C workstation (CH Instruments, USA). ORR was conducted in O_2-saturated 0.1 M KOH (Hg/HgO reference electrode) on the rotating-disk electrode system (Pine Research Instrumentation, USA). The durability of N-graphene and Pt/C (ETek, 20%Pt) toward oxygen reduction was tested with an accelerated degradation test (ADT) protocol: 1000 cyclic voltammograms (CVs) (−0.3∼0.3 V *vs.* Hg/HgO) in N_2-saturated 0.1 M KOH (50 mV/s). The CVs and the current–time curves of the electrocatalytic reduction of H_2O_2 were carried out in 10 mM PBS + 100 mM KCl (pH = 7.4) with a certain amount of H_2O_2 added. A Ag/AgCl reference electrode was used. The sample solutions were purged with ultrapure nitrogen for at least 30 min to remove oxygen before H_2O_2 reduction experiments.

The ORR kinetic currents (I_k) were calculated using the mass-transport correction Koutecky–Levich eqn (1):[52]

$$I_k = \frac{I_d \times I}{I_d - I} \quad (1)$$

where I_k = experimentally obtained ORR current at a certain potential, and I_d = experimentally measured diffusion-limited current.

3. Results and discussion

Fig. 1a shows the ORR kinetic currents before and after the accelerated degradation test (ADT), which were calculated, using the Koutecky–Levich equation, from ORR polarization curves on graphene, N-graphene, and Pt/C (ETek, 20wt%) electrodes (see Fig. S2†). The ADT was carried out with potential cycling between −0.3 V and 0.3 V (Hg/HgO) which mimics the potential range of oxygen electrodes in alkaline fuel cells (with the increasing interest in alkaline fuel cells,[53,54] we tested the electrocatalytic activity of N-graphene in alkaline medium). ORR kinetic currents for graphene, N-graphene and Pt/C at −0.03 V (Hg/HgO) are ∼1, 65, and 255 μA, respectively. The polarization curves (Fig. S2†) show that the ORR overpotential is greatly decreased on N-graphene in comparison with graphene. These indicate that nitrogen doping greatly increases the electrocatalytic activity of graphene towards ORR. N-graphene exhibits a lower initial electrocatalytic activity than Pt/C, but it has much higher durability than Pt/C. After ADT, N-graphene exhibits a slight increase in ORR activity (kinetic currents), however, Pt/C degraded by ∼85% in ORR activity. After ADT, N-graphene exhibits higher activity than Pt/C (Fig. 1a)! This indicates the possibility of replacing expensive Pt with low-cost N-graphene. The performance degradation of Pt/C is mainly attributed to the sintering of Pt nanoparticles[23,48] which can be seen from CVs on Pt/C before and after ADT (Fig. 1b): the wavelike bands in the potential range (−0.9∼−0.4 V) that are attributed to hydrogen adsorption/desorption[23] are greatly suppressed after ADT which means that the electrochemically active surface area of Pt is

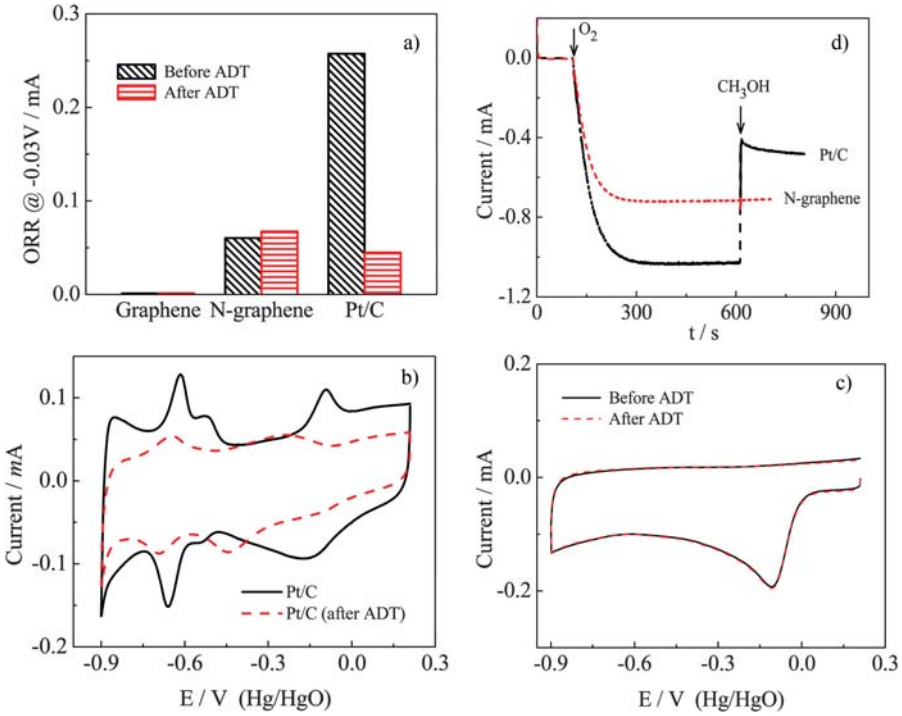

Fig. 1 (a) ORR currents at −0.03 V (Hg/HgO) (data calculated from Fig. S2 using Koutecky–Levich eqn (1)); (b) CVs on Pt/C in N_2-saturated 0.1 M KOH (50 mV/s); (c) CVs on N-graphene in O_2-saturated 0.1 M KOH (50 mV/s); (d) *I–t* chronoamperometric responses at −0.3 V (Hg/HgO) in N_2-saturated 0.1 M KOH on N-graphene and Pt/C electrodes (1600 rpm) followed by introducing O_2 and CH_3OH (0.3 M). ADT (accelerated degradation test): 1000 CVs (−0.3∼0.3 V *vs.* Hg/HgO) in N_2-saturated 0.1 M KOH (50 mV/s).

largely decreased.[55] However, CVs on N-graphene in O_2-saturated 0.1 M KOH show no changes before and after ADT (Fig. 1c), which indicates no changes in surface chemistry and high stability of N-graphene. Another advantage of N-graphene over Pt as an ORR electrocatalyst is that oxygen reduction on N-graphene is not influenced by fuel molecules (*e.g.*, methanol) as Pt is (Fig. 1d). In a methanol fuel cell, methanol crossover from anode to cathode could diminish cathodic performance through the depolarizing effect.[23] The high selectivity of N-graphene toward ORR makes it very promising in direct liquid fuel cells.

Fig. 2a shows the electrocatalytic reduction of H_2O_2 on graphene and N-graphene electrodes. The onset potentials of H_2O_2 reduction are −130 mV and 0 mV (Ag/AgCl) for graphene and N-graphene electrodes, respectively, *i.e.*, the overpotential is greatly decreased on N-graphene. There is a well-defined and greatly enhanced H_2O_2 reduction peak around −0.2 V in the CV on N-graphene. These indicate the superior electrocatalytic activity of N-graphene toward H_2O_2 reduction. Fig. 2b shows the amperometric responses at −0.2 V on graphene and N-graphene electrodes with successive addition of 0.1 mM H_2O_2. The enhanced current signal on the N-graphene electrode reveals the high electrocatalytic activity of N-graphene, consistent with the voltammetric studies (Fig. 2a). The linear relationship of H_2O_2 on the N-graphene electrode (Fig. 2b, inset) is 10^{-5} mM–2.8 mM, much wider than that for graphene (10^{-4} mM–1.8 mM) in this

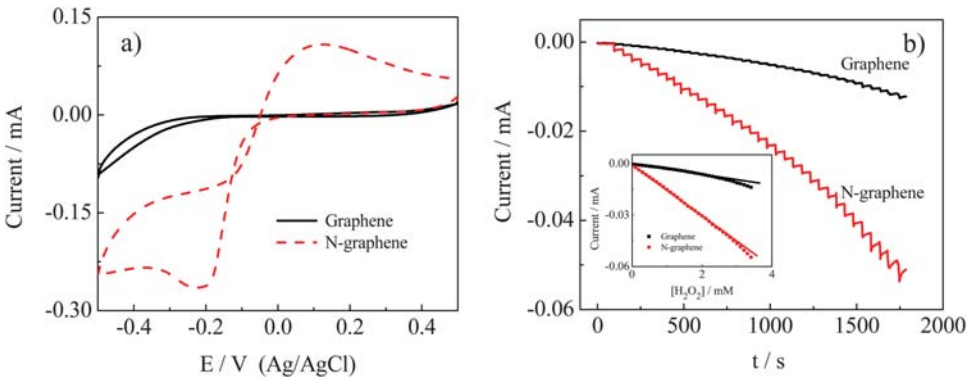

Fig. 2 (a) CVs (50 mV/s, background-subtracted) of H_2O_2 reduction on graphene and N-graphene in N_2-saturated 5 mM H_2O_2 + 10 mM PBS + 100 mM KCl (pH = 7.4). b) *I–t* chronoamperometric responses on graphene and N-graphene at −0.2 V (Ag/AgCl) in N_2-saturated 10 mM PBS + 100 mM KCl (pH = 7.4) with successive addition of 0.1 mM H_2O_2 (inset: calibration curves of H_2O_2 reduction).

work and previously reported chemically-reduced graphene oxide (5×10^{-5} mM–1.5 mM).[27] Therefore, N-graphene exhibits excellent performance in sensing H_2O_2.

It has been shown that nitrogen doping of carbon nanostructures improves their electrocatalytic activity.[23,24] Fig. 3a shows the XPS spectra of doped/undoped graphene in the N1s binding energy (BE) range and Fig. 3b shows XPS spectra of doped/undoped graphene in the O1s BE range. The XPS spectra are fitted to get detailed chemical bonding information of the elements N and O with carbon (see Table 1 for the fitted results). Nitrogen is observed in N-graphene, confirming its incorporation into graphene. Generally, there are several nitrogen functional groups in nitrogen-doped carbon. These include pyridinic-N (N1, BE = 398.7 ± 0.2 eV), pyrrolic-N (N2, BE = 400.3 ± 0.2 eV), quaternary nitrogen (N3, BE = 401.2 ± 0.2 eV), and N-oxides of pyridinic-N (N4, BE = 402.8 ± 0.4 eV).[56–58] The nitrogen functional groups are usually in the following molecular structures (chemical states):[56,58] pyridinic-N (labeled as N1) refers to nitrogen atoms at the edge of graphene planes, each of which is bonded to two carbon atoms and donates one p-electron to the aromatic π system; pyrrolic-N (labeled as N2) refers to nitrogen atoms that are bonded to two carbon atoms and contribute to the π system with two p-electrons; quaternary nitrogen (labeled as N3) is also called "graphitic nitrogen" or "substituted nitrogen", in which nitrogen atoms are incorporated into the graphene layer and replace carbon atoms within a graphene plane; N-oxides of pyridinic-N (labeled as N4, pyridinic–(N^+–O^-)) are bonded to two carbon atoms and one oxygen atom. The role of the real "electrocatalytically active sites" is still controversial since their contribution to the catalytic activity is not well defined.[24] In some studies, the enhanced electrocatalytic activity is attributed to pyridinic-N and/or pyrrolic-N.[56,59] A recent study[60] suggests that graphitic nitrogen is more important for the electrocatalytic activity of nitrogen-doped carbon. Our XPS results indicate that N-graphene contains all these three functional groups (pyridinic-N, pyrrolic-N, and graphitic-N). It is believed that carbon atoms adjacent to nitrogen dopants possess a substantially higher positive charge density to counterbalance the strong electronic affinity of the nitrogen atom,[23] which results in an enhanced adsorption of O_2 and reactive intermediates (*i.e.*, superoxide, hydroperoxide) that proceeds to accelerate the ORR.[59] The nitrogen-induced charge delocalization could also change the chemisorption mode of O_2 from monoatomic end-on adsorption on undoped carbon to a diatomic side-on adsorption at nitrogen-doped carbon which effectively weakens the O–O bond to facilitate ORR.[23] This is also true for H_2O_2 reduction because breaking the O–O bond is also a key step for electrocatalytic reduction of H_2O_2. And the presence of nitrogen enhances the ability of graphene sheets to donate electrons,[57] which is advantageous for reduction reactions.

In addition to incorporating nitrogen into graphene, N_2 plasma treatment also creates structural defects on graphene with an increased amount of unsaturated carbon atoms at graphene edge sites which are very active to react with oxygen and form oxygen-containing groups when exposed to air.[61] The structure defects[62] and oxygen-containing groups[63] might also catalyze the reduction of oxygen and H_2O_2 (oxygen plasma treated graphene, which has similar oxygen functional groups as N-graphene, exhibits higher electrocatalytic activity toward both oxygen reduction and H_2O_2 reduction than graphene, but much lower than N-graphene; therefore, nitrogen doping controls the electrocatalytic activity,[64,65] see Table 1 and Supplementary Information† for more details). The structural defects and oxygen-containing groups are confirmed in O1s, C1s XPS spectra and Raman spectra. It can be seen that oxygen content increases after nitrogen plasma treatment, and oxygen atoms are bonded with carbon in the form of C–O, C═O, and O–C═O (Fig. 3b, Table 1).[66] Fig. 4 shows the Raman spectra of graphene and N-graphene. The two peaks are attributed to the G band at 1594 cm^{-1} and D band at 1348 cm^{-1}, respectively. The G band is related to the in-plane bond-stretching motion of pairs of sp^2-C atoms.[67–70] The D band ("disordered" band) is the breathing mode of the sp^2-rings of the graphene layer that is related to a series of defects: bond-angle disorder, bond-length disorder, and hybridization[68] which are caused by heteroatom (nitrogen/oxygen) doping and structure defects by plasma treatment.[67,69,71] Therefore, the relatively increased intensity of the D band for N-graphene (Fig. 4) indicates that the content of disordered carbon increases after plasma treatment, mainly by nitrogen doping.[44,71]

In summary, we present the excellent electrochemical properties of nitrogen-doped graphene. N-graphene was synthesized by exposing graphene to nitrogen plasma. N-graphene exhibits much higher electrocatalytic activity toward oxygen reduction and H_2O_2 reduction than graphene, and much higher durability

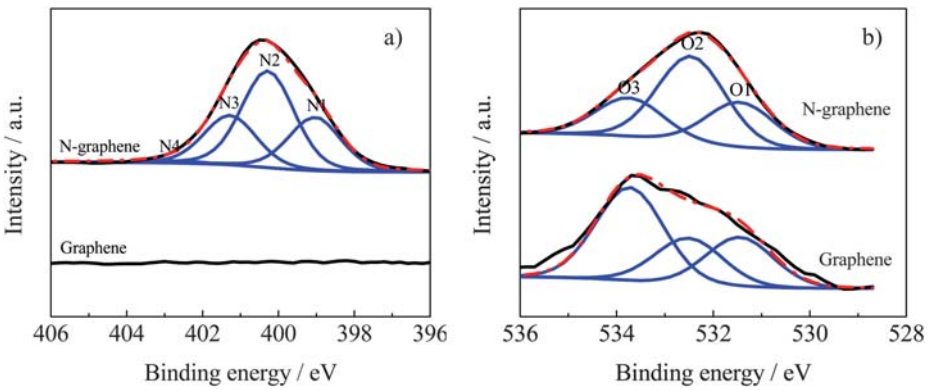

Fig. 3 Core level high-resolution N1s (a) and O1s (b) XPS spectra of graphene and N-graphene.

Table 1 Fitted results of N1s and O1s core level XPS spectra of graphene, O-graphene and N-graphene[a]

	Element content/at%			Nitrogen functional groups/(BE, eV)				Oxygen functional groups/(BE, eV)		
Samples	C	O	N	N4(402.8)	N3(401.1)	N2(400.3)	N1(399.0)	O3(533.8)	O2(532.6)	O1(531.5)
Graphene	96.5	3.5	0	—	—	—	—	49.3	24.5	26.2
O-graphene	88.4	11.2	0.4	—	—	—	—	28.4	48.9	22.7
N-graphene	82.9	8.6	8.5	1.0	24.0	48.5	26.5	19.9	44.9	35.2

[a] Notes. N1: pyridinic-N, N2: pyrrolic-N, N3: quarternary/graphitic-N, N4: pyridinic–(N^+–O^-), O1: O–C, O2: O=C, O3: O–C=O.

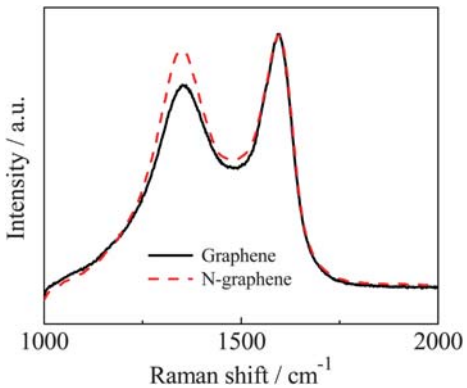

Fig. 4 Raman spectra of graphene and N-graphene.

and selectivity than the widely-used and expensive Pt. The enhanced performance is mainly attributed to nitrogen functional groups in N-graphene. The structure defects and oxygen-containing groups also contribute to the enhanced electrocatalytic activity of N-graphene. N-graphene is promising for applications in electrochemical energy devices (fuel cells, metal–air batteries) and biosensors.

Acknowledgements

This work is supported by a Laboratory Directed Research and Development program at Pacific Northwest National Laboratory (PNNL). The characterization was performed using EMSL, a national scientific user facility sponsored by the DOE's Office of Biological and Environmental Research and located at PNNL. PNNL is operated for the DOE by Battelle under Contract DE-AC05-76RL01830. SZ acknowledges a fellowship from the China Scholarship Council to perform this work at PNNL. IAA acknowledges support from ARRA/AFOSR under Grant No. FA9550-09-1-0523 and ARO MURI under Contract No. W911NF-04-1-0178.

References

1 A. K. Geim and K. S. Novoselov, *Nat. Mater.*, 2007, **6**, 183–191.
2 C. Lee, X. D. Wei, J. W. Kysar and J. Hone, *Science*, 2008, **321**, 385–388.
3 H. C. Schniepp, J. L. Li, M. J. McAllister, H. Sai, M. Herrera-Alonso, D. H. Adamson, R. K. Prud'homme, R. Car, D. A. Saville and I. A. Aksay, *J. Phys. Chem. B*, 2006, **110**, 8535–8539.
4 F. Chen, J. L. Xia, D. K. Ferry and N. J. Tao, *Nano Lett.*, 2009, **9**, 2571–2574.
5 M. D. Stoller, S. J. Park, Y. W. Zhu, J. H. An and R. S. Ruoff, *Nano Lett.*, 2008, **8**, 3498–3502.
6 X. Wang, L. J. Zhi, N. Tsao, Z. Tomovic, J. L. Li and K. Mullen, *Angew. Chem., Int. Ed.*, 2008, **47**, 2990–2992.
7 E. Yoo, T. Okata, T. Akita, M. Kohyama, J. Nakamura and I. Honma, *Nano Lett.*, 2009, **9**, 2255–2259.
8 R. Kou, Y. Y. Shao, D. H. Wang, M. H. Engelhard, J. H. Kwak, J. Wang, V. V. Viswanathan, C. M. Wang, Y. H. Lin, Y. Wang, I. A. Aksay and J. Liu, *Electrochem. Commun.*, 2009, **11**, 954–957.
9 D. H. Wang, D. W. Choi, J. Li, Z. G. Yang, Z. M. Nie, R. Kou, D. H. Hu, C. M. Wang, L. V. Saraf, J. G. Zhang, I. A. Aksay and J. Liu, *ACS Nano*, 2009, **3**, 907–914.
10 Z. Liu, J. T. Robinson, X. M. Sun and H. J. Dai, *J. Am. Chem. Soc.*, 2008, **130**, 10876–10877.
11 C. S. Shan, H. F. Yang, J. F. Song, D. X. Han, A. Ivaska and L. Niu, *Anal. Chem.*, 2009, **81**, 2378–2382.
12 C. H. Lu, H. H. Yang, C. L. Zhu, X. Chen and G. N. Chen, *Angew. Chem., Int. Ed.*, 2009, **48**, 4785–4787.
13 Y. Y. Shao, J. Wang, H. Wu, J. Liu, I. A. Aksay and Y. H. Lin, *Electroanalysis*, 2010, **22**, 1027–1036.
14 Y. F. Li, Z. Zhou, P. W. Shen and Z. F. Chen, *ACS Nano*, 2009, **3**, 1952–1958.
15 D. W. Boukhvalov and M. I. Katsnelson, *Nano Lett.*, 2008, **8**, 4373–4379.
16 X. R. Wang, X. L. Li, L. Zhang, Y. Yoon, P. K. Weber, H. L. Wang, J. Guo and H. J. Dai, *Science*, 2009, **324**, 768–771.
17 D. C. Wei, Y. Q. Liu, Y. Wang, H. L. Zhang, L. P. Huang and G. Yu, *Nano Lett.*, 2009, **9**, 1752–1758.
18 X. L. Li, H. L. Wang, J. T. Robinson, H. Sanchez, G. Diankov and H. J. Dai, *J. Am. Chem. Soc.*, 2009, **131**, 15939–15944.
19 L. S. Panchakarla, K. S. Subrahmanyam, S. S. K., A. Govindaraj, H. R. Krishnamurthy, U. V. Waghmare and C. N. R. Rao, *Adv. Mater.*, 2009, **21**, 4726–4730.
20 L. T. Qu, Y. Liu, J. B. Baek and L. M. Dai, *ACS Nano*, 2010, **4**, 1321.
21 X. L. Li, X. R. Wang, L. Zhang, S. W. Lee and H. J. Dai, *Science*, 2008, **319**, 1229–1232.
22 C. P. Ewels and M. Glerup, *J. Nanosci. Nanotechnol.*, 2005, **5**, 1345–1363.
23 K. P. Gong, F. Du, Z. H. Xia, M. Durstock and L. M. Dai, *Science*, 2009, **323**, 760–764.
24 Y. Y. Shao, J. H. Sui, G. P. Yin and Y. Z. Gao, *Appl. Catal., B*, 2008, **79**, 89–99.
25 S. Y. Deng, G. Q. Jian, J. P. Lei, Z. Hu and H. X. Ju, *Biosens. Bioelectron.*, 2009, **25**, 373–377.
26 Z. Wang, X. Zhou, J. Zhang, F. Boey and H. Zhang, *J. Phys. Chem. C*, 2009, **113**, 14071–14075.
27 M. Zhou, Y. M. Zhai and S. J. Dong, *Anal. Chem.*, 2009, **81**, 5603–5613.
28 S. Alwarappan, A. Erdem, C. Liu and C. Z. Li, *J. Phys. Chem. C*, 2009, **113**, 8853–8857.
29 N. G. Shang, P. Papakonstantinou, M. McMullan, M. Chu, A. Stamboulis, A. Potenza, S. S. Dhesi and H. Marchetto, *Adv. Funct. Mater.*, 2008, **18**, 3506–3514.
30 F. H. Li, H. F. Yang, C. S. Shan, Q. X. Zhang, D. X. Han, A. Ivaska and L. Niu, *J. Mater. Chem.*, 2009, **19**, 4022–4025.
31 L. H. Tang, Y. Wang, Y. M. Li, H. B. Feng, J. Lu and J. H. Li, *Adv. Funct. Mater.*, 2009, **19**, 2782–2789.
32 S. Park and R. S. Ruoff, *Nat. Nanotechnol.*, 2009, **4**, 217–224.
33 K. S. Novoselov, A. K. Geim, S. V. Morozov, D. Jiang, Y. Zhang, S. V. Dubonos, I. V. Grigorieva and A. A. Firsov, *Science*, 2004, **306**, 666–669.
34 Y. Hernandez, V. Nicolosi, M. Lotya, F. M. Blighe, Z. Y. Sun, S. De, I. T. McGovern, B. Holland, M. Byrne, Y. K. Gun'ko, J. J. Boland,

P. Niraj, G. Duesberg, S. Krishnamurthy, R. Goodhue, J. Hutchison, V. Scardaci, A. C. Ferrari and J. N. Coleman, *Nat. Nanotechnol.*, 2008, **3**, 563–568.
35 A. Reina, X. T. Jia, J. Ho, D. Nezich, H. B. Son, V. Bulovic, M. S. Dresselhaus and J. Kong, *Nano Lett.*, 2009, **9**, 30–35.
36 S. Stankovich, D. A. Dikin, R. D. Piner, K. A. Kohlhaas, A. Kleinhammes, Y. Jia, Y. Wu, S. T. Nguyen and R. S. Ruoff, *Carbon*, 2007, **45**, 1558–1565.
37 S. Gilje, S. Han, M. Wang, K. L. Wang and R. B. Kaner, *Nano Lett.*, 2007, **7**, 3394–3398.
38 Y. Y. Shao, J. Wang, M. Engelhard, C. M. Wang and Y. H. Lin, *J. Mater. Chem.*, 2010, **20**, 743–748.
39 W. Qian, R. Hao, Y. L. Hou, Y. Tian, C. M. Shen, H. J. Gao and X. L. Liang, *Nano Res.*, 2009, **2**, 706–712.
40 N. Li, Z. Y. Wang, K. K. Zhao, Z. J. Shi, Z. N. Gu and S. K. Xu, *Carbon*, 2010, **48**, 255–259.
41 L. S. Panchokarla, K. S. Subrahmanyam, S. K. Saha, A. Govindaraj, H. R. Krishnamurthy, U. V. Waghmare and C. N. R. Rao, *Adv. Mater.*, 2009, **21**, 4726–4730.
42 L. T. Qu, Y. Liu, J. B. Baek and L. M. Dai, *ACS Nano*, 2010, **4**, 1321–1326.
43 M. J. McAllister, J. L. Li, D. H. Adamson, H. C. Schniepp, A. A. Abdala, J. Liu, M. Herrera-Alonso, D. L. Milius, R. Car, R. K. Prud'homme and I. A. Aksay, *Chem. Mater.*, 2007, **19**, 4396–4404.
44 K. N. Kudin, B. Ozbas, H. C. Schniepp, R. K. Prud'homme, I. A. Aksay and R. Car, *Nano Lett.*, 2008, **8**, 36–41.
45 Y. Y. Shao, G. P. Yin and Y. Z. Gao, *J. Power Sources*, 2007, **171**, 558–566.
46 H. A. Gasteiger and N. M. Markovic, *Science*, 2009, **324**, 48–49.
47 Z. W. Chen, M. Waje, W. Z. Li and Y. S. Yan, *Angew. Chem., Int. Ed.*, 2007, **46**, 4060–4063.
48 J. Zhang, K. Sasaki, E. Sutter and R. R. Adzic, *Science*, 2007, **315**, 220–222.
49 W. Chen and S. W. Chen, *Angew. Chem., Int. Ed.*, 2009, **48**, 4386–4389.
50 J. Wang, *Electroanalysis*, 2005, **17**, 7–14.
51 P. N. Nirmalraj, P. E. Lyons, S. De, J. N. Coleman and J. J. Boland, *Nano Lett.*, 2009, **9**, 3890–3895.
52 H. A. Gasteiger, S. S. Kocha, B. Sompalli and F. T. Wagner, *Appl. Catal., B*, 2005, **56**, 9–35.
53 S. Gu, R. Cai, T. Luo, Z. W. Chen, M. W. Sun, Y. Liu, G. H. He and Y. S. Yan, *Angew. Chem., Int. Ed.*, 2009, **48**, 6499–6502.
54 S. F. Lu, J. Pan, A. B. Huang, L. Zhuang and J. T. Lu, *Proc. Natl. Acad. Sci. U. S. A.*, 2008, **105**, 20611–20614.
55 Y. Y. Shao, G. P. Yin, Y. Z. Gao and P. F. Shi, *J. Electrochem. Soc.*, 2006, **153**, A1093–A1097.
56 P. H. Matter, L. Zhang and U. S. Ozkan, *J. Catal.*, 2006, **239**, 83–96.
57 S. Kundu, T. C. Nagaiah, W. Xia, Y. Wang, S. V. Dommele, J. H. Bitter, M. Santa, G. Grundmeier, M. Bron, W. Schuhmann and M. Muhler, *J. Phys. Chem. C*, 2009, **113**, 14302–14310.
58 R. Arrigo, M. Havecker, R. Schlogl and D. S. Su, *Chem. Commun.*, 2008, 4891–4893.
59 S. Maldonado and K. J. Stevenson, *J. Phys. Chem. B*, 2005, **109**, 4707–4716.
60 H. Niwa, K. Horiba, Y. Harada, M. Oshima, T. Ikeda, K. Terakura, J. Ozaki and S. Miyata, *J. Power Sources*, 2009, **187**, 93–97.
61 G. Abbas, P. Papakonstantinou, G. R. S. Iyer, I. W. Kirkman and L. C. Chen, *Phys. Rev. B: Condens. Matter Mater. Phys.*, 2007, **75**, 195429.
62 C. E. Banks, T. J. Davies, G. G. Wildgoose and R. G. Compton, *Chem. Commun.*, 2005, 829–841.
63 E. Yeager, *J. Mol. Catal.*, 1986, **38**, 5–25.
64 F. Jaouen, S. Marcotte, J. P. Dodelet and G. Lindbergh, *J. Phys. Chem. B*, 2003, **107**, 1376–1386.
65 E. J. Biddinger, D. von Deak and U. S. Ozkan, *Top. Catal.*, 2009, **52**, 1566–1574.
66 B. Khare, P. Wilhite, B. Tran, E. Teixeira, K. Fresquez, D. N. Mvondo, C. Bauschlicher and M. Meyyappan, *J. Phys. Chem. B*, 2005, **109**, 23466–23472.
67 A. C. Ferrari, *Solid State Commun.*, 2007, **143**, 47–57.
68 A. C. Ferrari and J. Robertson, *Phys. Rev. B: Condens. Matter Mater. Phys.*, 2000, **61**, 14095–14107.
69 M. A. Pimenta, G. Dresselhaus, M. S. Dresselhaus, L. G. Cancado, A. Jorio and R. Saito, *Phys. Chem. Chem. Phys.*, 2007, **9**, 1276–1291.
70 F. Tuinstra and J. L. Koenig, *J. Chem. Phys.*, 1970, **53**, 1126–1130.
71 M. J. Allen, J. D. Fowler, V. C. Tung, Y. Yang, B. H. Weiller and R. B. Kaner, *Appl. Phys. Lett.*, 2008, **93**, 193119.

